LA-UR-99-3551
Approved for public release;
distribution is unlimited.

Title: **SPALLATION STUDIES ON SHOCK LOADED U-6 WT PCT NB**

Author(s): D.L. Tonks, J. E. Vorthman, R. Hixson, A. Kelly, and A. K. Zurek

Submitted to:

http://lib-www.lanl.gov/la-pubs/00796064.pdf

SPALLATION STUDIES ON SHOCK LOADED U-6 WT PCT NB

D.L. Tonks, J. E. Vorthman, R. Hixson, A. Kelly, and A. K. Zurek

Los Alamos National Laboratory, Los Alamos, NM 87545.

Abstract. Several spallation experiments have been performed on the 6 wt pct alloy of uranium using gas gun driven normal plate impacts with VISAR instrumentation and soft recovery. The nominal shock pressures achieved were 28, 34, 42, 50, 55, and 82 kbar. This paper will focus on spallation modeling, e. g. using the 1 D characteristics code CHARADE to simulate the free surface particle velocity. The spallation model involves the ductile growth and coalescence of voids. Metallographical examination of recovered samples and details of the experimental apparatus are discussed in a separate paper.

INTRODUCTION

To our knowledge, no comprehensive study of spallation has been done for the 6 wt pct Nb alloy. Recently, we have performed gas gun plate impact experiments on this alloy with VISAR measurement of the free surface velocity and soft recovery of samples. Shock strengths induced were nominally 28, 34, 42, 50, 55, and 82 kbar. The details of the gas gun work and of the metallurgical examinations are presented in another paper in this volume. (1)

In this paper, the free surface velocity and spallation behavior are modeled using the 1D hydrocode CHARADE (2) with a simple ductile void growth spallation model. The modeling is mostly successful but should be improved, a likely improvement being twinning plasticity.

SPALLATION AND MATERIALS MODELING

Before presenting the spallation model, the equation of state and plasticity modeling will be briefly described. The equation of state (eos) treatment is patterned after the "almost isotropic" approximation of Wallace(3). A "pressure dependent bulk modulus" for use in this treatment was obtained from Marsh's U-6% Nb Hugoniot relation (4) in the usual way: $U_s = 2.56(mm/\mu s) + 1.55U_p$, where U_s is the shock velocity and U_p is the particle velocity. The elastic moduli were degraded because of damage using a simple rule of mixtures.

Part of the eos model assumptions is that of a constant Poisson's ratio, ν, for which value 0.39 was used. This value is based on three sets of sound speed measurements taken by us and Marsh (4) under ambient conditions. The measured longitudinal sound speeds are 2.96, 2.95, and 2.90 mm/μs, for our two sets and Marsh's set. The measured shear sound velocities are 1.31, 1.27, and 1.23, respectively. The measured densities are 17.44, 17.42, and 17.411, gm/cm^3 . The Poisson ratio values calculated from the three data sets are 0.38, 0.39, and 0.39, respectively. The calculated shear modulus values are 299, 281, and 263 kbar, respectively. The calculated Young's modulus values are 825, 779, and 732 kbar, respectively.

The bulk sound velocities obtained from the above elastic constants are 2.544, 2.56, and 2.53, mm/μsec, respectively, for our two sets and Marsh's data set. These values compare quite favorably with the

constant, 2.56 mm/μsec, in Marsh's $U_s - U_p$ relation. These results suggest that our two materials are quite similar to Marsh's material, and that Marsh's $U_s - U_p$ relation is quite appropriate for our two materials.

It is important to know the fabrication heat treatment for U-6% Nb samples, since the mechanical behavior varies widely, for example, for aged samples. Our material was obtained from Rocky Flats in the "soft" condition, i. e. fast quenched from the $gamma_1$ state into the martensitic α" + γ_o phase mixture. The elastic constant values discussed above are compatible with the data from this state given in Ref. (5).

The deviatoric plasticity model, used for both forward and backward plasticity, which was not degraded by damage, was the following: $\dot{\psi} = \dot{\psi}_o(\tau - \tau_{y,i})^2$ where $\dot{\psi}$ is the effective plastic strain rate, τ is the von Mises effective deviatoric stress, and $\tau_{y,i}$ is the yield stress , i=f and i = b indicating the forward and backward yield stress, respectively.

A ductile void growth model was used for the

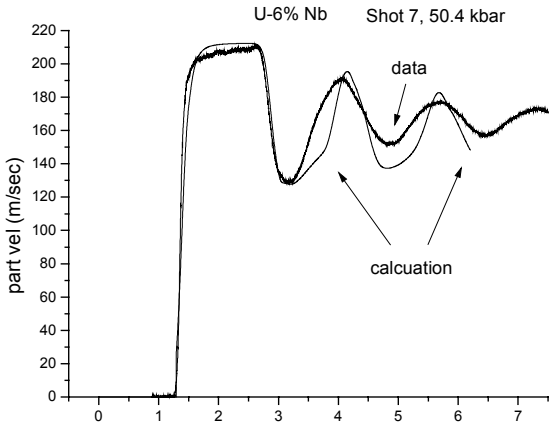

FIGURE 1. Calculated and measured free surface particle velocity profiles, which are shifted in time for best overlap.

damage evolution. This choice was made because standard tensile fracture tests (6) show such behavior. Unfortunately, the only recovered sample examined to date, that of shot 19, involved an impact too weak to show the nature of damage growth beyond carbide cracking. The model used for the porosity growth rate $\dot{\rho}$ is:

$$\dot{\rho}/\rho(1-\rho) = 1.5\dot{\varepsilon}_o\left[(-\tfrac{3}{2}P + y\ln\rho)/[\sigma_o n(1-\rho^{1/n})]\right]^n \qquad (1),$$

where $\dot{\varepsilon}_o$ and σ_o are material strain rate and stress parameters that occur in the following law for the plastic strain rate in the matrix surrounding the growing void: $\dot{\psi} = \dot{\varepsilon}_o[(\tau - y)/\sigma_o]^n$. P is the pressure. This formula is the pressure only limit of a relation derived earlier.[7] The fracture criteria used is a porosity spall limit beyond which a computational cell does not support stress.

The void growth formula (1) above has a different plasticity law than that used for the matrix. This is reasonable since the region around the growing voids experiences a much different path than that of the matrix, e. g. much higher temperatures and strain rates. A significant feature of the formula (1) is a "pressure threshold" of (2/3)y ln ρ for void growth. P must be lower than this (P is negative for void growth), before void growth can occur. This threshold corresponds roughly to the "spall Pressure" of the "P_{min}" spallation model, in which fracture of a computational cell occurs for pressures lower than P_{min}.

RESULTS

In order to obtain a rough idea of the spall behavior, the P_{min} model was used to calculate P_{min} values by fitting the lowest dip in the VISAR data. See Table 1. In this model, no eos degradation was used and no damage evolution occurred. These P_{min} values are generally lower, i. e. bigger in size, than the peak minimum pressures that occurred in the full damage model calculations. For example, the peak minimum pressures for the damage calculations of shots 9 and 21 were –22 and –26 kbar, respectively, while the corresponding P_{min} values were -27 and -36 kbar.

TABLE 1. Tensile threshold model spall strengths

Shot #	**Shock Strength**	$-\lvert P_{min}\rvert$
56-98- 7	50.4 kbar	31 kbar
56-98- 9	34 kbar	27 kbar
56-99-12	82 kbar	33.5 kbar
56-99-19	28 kbar	n/a
56-99-21	55 kbar	36 kbar
56-99-27	42 kbar	33 kbar

The CHARADE full damage model results presented in the following figures 1-4 generally

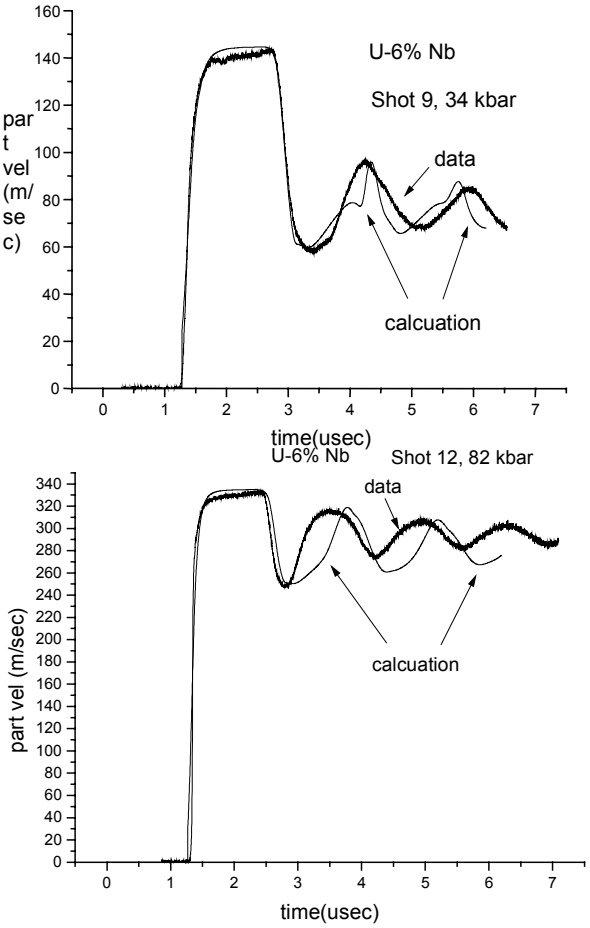

FIGURE 2. Calculated and measured free surface particle velocity profiles.

capture successfully the behavior near the spall dip. Hence, the damage initiation and part of the subsequent damage growth are modeled well. In particular, most of the VISAR trace of the weakest impact, in Fig. 3, in which mostly inclusion cracking occurred, is successfully modeled. For the stronger impacts, the smooth rise and turn over after the spall dip is not modeled well. The sudden peak in the calculated turn over for shot 9, for example, is caused by the achievement of fracture. The measured peak height is achieved in the calculation, so the overall dissipation in the model is correct, but the details of late damage evolution and the transition to fracture are not modeled so well. This is probably due to not including the twinning plasticity that is known to occur at a few per cent strain in this alloy (8). Twinning plasticity is different from the generic "dislocation" plasticity in the model. Twinning plasticity modeling is a likely area of future progress.

The same set of full damage evolution parameters was used for all of the fits. The values used are: $\dot{\varepsilon}_o$ =5/μs, σ_o=6 kbar, y = 7 kbar, and n=1.5. The seed (initial) porosity, $\rho_{0,}$ is 0.02. and the spall porosity is 17.3 %. The large model seed porosity (whose value was not critical) corresponds well to the large inclusions, having a volume of about 1%, seen in the micrographs [1]. The initial value of –18.3 kbar of the "pressure threshold", (2/3)y ln ρ_o corresponds, in this modeling, which lacks an explicit void nucleation component, to the pressure to crack the carbides and nucleate a void. The y value, thus, is being made to serve two purposes, the void cracking and void growth. The model will be generalized to overcome this problem. The spallation porosity used is smaller than the 30% used for many fcc metals. We note that shot 27 is somewhat better modeled by changing n to 1.0, but the standard parameter set is close to the best for the other shots.

As mentioned earlier, this parameter set does best on the void nucleation and early damage evolution. Shot 19 is a good example, the recovered sample of which showed mostly void cracking.

The parameter values for the matrix power law plastic strain rate relation are as follows: $\dot{\psi}_o$ = $3x10^4$/s , τ_{yf} = 1.2 kbar , and τ_{yb}= 1.0 kbar. These two yield stresses are smaller but comparable to the yield stress of 2 kbar or more found in conventional low strain rate testing on different U6Nb material (9). Values of 2 kbar produce a noticeable calculated Hugoniot elastic limit, in disagreement with the VISAR data. Including twinning plasticity in the model might resolve this problem. However, it would have to be triggered in shock waves at a smaller stress than is seen in conventional mechanical testing (8).

REFERENCES

1. Vorthman, J. E., Hixson, R., Kelly, A., and Zurek, A. this volume.
2. Johnson, J. N., and Tonks, D. L. *, CHARADE: A Characteristic Code for Calculating Rate-Dependent Shock-Wave Response, LA-11993-MS* , Los Alamos National Laboratory, 1991
3. Wallace, D. C.*, Thermoelastic-Plastic Flow in Solids, LA-10119*, Los Alamos National Laboratory, 1985.
4. *LASL Shock Hugoniot Data*, edited by S. P. Marsh, Univ. of Calif. Press, 1980, Los Angeles, p. 229,
5. Lowry, D. R., Wolfenden, A., and Ludtka, G. M.*, Trans. ASME* **57**, 292 - 297 (1990).
6. Eckelmeyer, K. H., Romig, Jr., A. D., and Weirick, L. J.*, Met. Trans A* **15A**, 1319 - 1330 (1984).
7 Tonks, D. L., Zurek, A. K., and Thissell, W. R., in *Metallurgical and Materials Applications of Shock-Wave and High-Strain -Rate Phenomena*, edited by L. E. Murr, K. P. Staudhammer, and M. A. Meyers, Elsevier Science B. V., New York, 1995, pp. 171 - 178.
8. Govindjee, S., and Kasper, E. P. , *J. Intel. Mat. Sys. and Struc.* **8,** 815 - 823 (1997).
9. Gray, III, G. T., private communication.

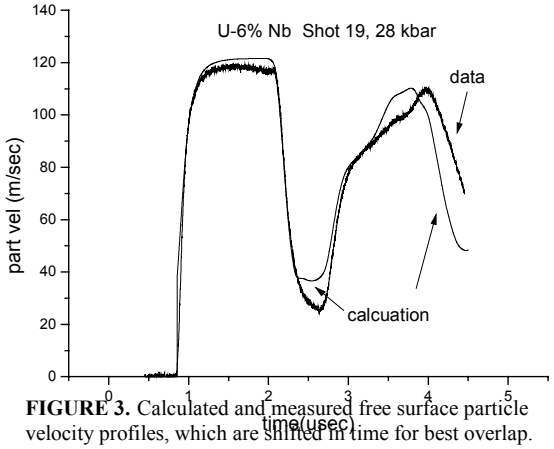

FIGURE 3. Calculated and measured free surface particle velocity profiles, which are shifted in time for best overlap.

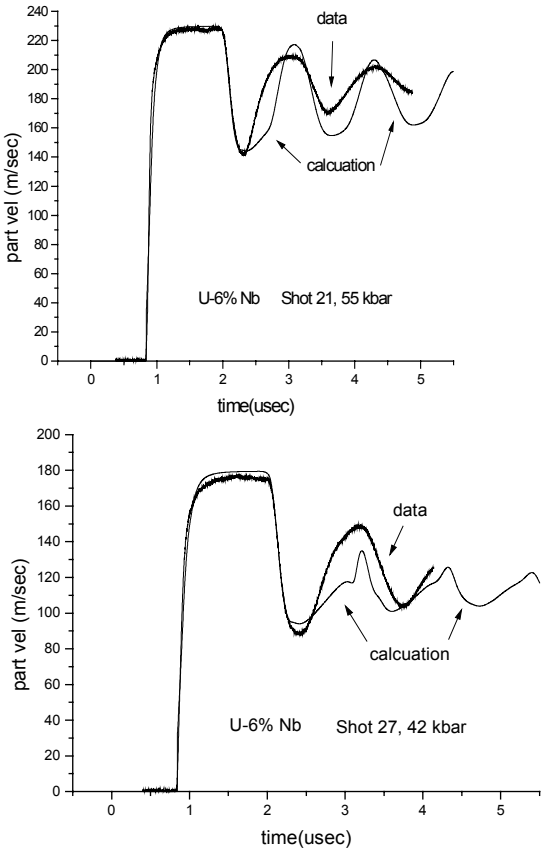

FIGURE 4. Calculated and measured free surface particle velocity profiles, which are shifted in time for best overlap.